# Magnetic field conditions upstream of Ganymede

Marissa F. Vogt[1], Fran Bagenal[2], and Scott J. Bolton[3]

[1] Center for Space Physics, Boston University, Boston, MA, USA

[2] Laboratory for Atmospheric and Space Physics, University of Colorado Boulder, Boulder, CO, USA

[3] Southwest Research Institute, San Antonio, TX, USA

Corresponding Author: Marissa Vogt, mvogt@bu.edu

## Key points

- The magnetic field magnitude and direction upstream of Ganymede vary strongly with longitude
- Temporal variations in the magnetosphere also influence Ganymede's upstream field conditions
- Juno's Ganymede flyby occurred during typical magnetospheric conditions

## Abstract

Jupiter's magnetic field is tilted by ~10º with respect to the planet's spin axis, and as a result the Jovian plasma sheet passes over the Galilean satellites at the jovigraphic equator twice per planetary rotation period. The plasma and magnetic field conditions near Ganymede's magnetosphere therefore change dramatically every ~5 hours, creating a unique magnetosphere-magnetosphere interaction, and on longer time scales as evidenced by orbit-to-orbit variations. In this paper we summarize the typical magnetic field conditions and their variability near Ganymede's orbit as observed by the Galileo and Juno spacecraft. We fit Juno data from orbit 34, which included the spacecraft's close Ganymede flyby in June 2021, to a current sheet model and show that the magnetospheric conditions during orbit 34 were very close to the historical average. Our results allow us to infer the upstream conditions at the time of the Juno Ganymede flyby.

**Plain Language Summary**

Ganymede is the only moon in the solar system with an intrinsic magnetic field. This field forms a bubble in space around the moon, called a magnetosphere, that is itself contained within Jupiter's magnetosphere. The magnetic field and plasma conditions within Ganymede's magnetosphere can be used to infer information about the satellite's atmosphere, ionosphere, and interior. It is therefore important to understand the interaction between Ganymede's magnetosphere and the Jovian environment in the same way that we study the effects of space weather on the Earth. Here we analyze Galileo magnetic field measurements from Jupiter's magnetosphere in the region near Ganymede's orbit to establish the typical magnetic field magnitude and direction. We discuss the average conditions as well as the nature of the variability that occurs due to dynamic processes occurring in Jupiter's magnetosphere. This information provides useful context for analyzing data from Juno's recent flyby of Ganymede, which we show occurred during typical magnetospheric conditions.

## 1. Introduction

Jupiter's moon Ganymede is the only satellite in the solar system to possess its own intrinsic magnetic field, which creates a small magnetosphere that is embedded in Jupiter's inner magnetosphere (Kivelson et al., 1996). Ganymede is therefore a fascinating target for studying moon-magnetosphere interactions. Data and models from the Galileo flybys of Io, Europa, Ganymede, and Callisto show that changes in the upstream conditions, including the satellite's location with respect to Jupiter's plasma sheet, can have a major influence on the moon-magnetosphere interaction and produce an inductive response that can be used to probe the moons' internal structure (e.g. Kivelson et al., 1999, 2002). The observed magnetic field from within Ganymede's magnetosphere contains contributions from Ganymede's internal magnetic field, currents within Ganymede's magnetosphere, any inductive magnetic field from a possible subsurface liquid ocean inside the moon, and the magnetic field of Jupiter's magnetosphere (Kivelson et al., 2002). Therefore, it is important to quantify the range of magnetic field and plasma conditions that may be expected upstream of the Galilean satellites and to predict those conditions at the time of close spacecraft encounters.

The goals of this paper are 1) to establish the range of likely magnetic field conditions upstream of Ganymede by analyzing the available Galileo and Juno magnetometer data, and 2) to examine the magnetic field conditions near Ganymede during Juno's orbit 34 prior to and following its close flyby of Ganymede on 7 June 2021. We first consider how the magnetic field magnitude and direction near Ganymede change over the ~10 hour planetary rotation period as the satellite's magnetic latitude oscillates due to Jupiter's ~10º dipole tilt. We then consider how the magnetic field conditions change on longer timescales such as the orbit-by-orbit current sheet variability that has been studied in both Galileo and Juno data (e.g. Russell et al., 2001; Vogt et al., 2017; Connerney et al., 2020). Both of these types of variability in the upstream conditions occur on timescales that are long compared to the ~minutes long timescale for plasma circulation in Ganymede's magnetosphere (e.g. Jia et al., 2009, 2010; Toth et al., 2016; Zhou et al., 2020) and it is likely that conditions are always favorable for magnetopause reconnection (Kaweeyanun et al., 2020). But even if the upstream field conditions have only a limited influence on activity in Ganymede's magnetosphere, they can still affect the interpretation of magnetic field measurements near Ganymede. In particular, the magnetic field observed near Ganymede includes the contributions of both Jupiter's magnetosphere field and the field produced by Ganymede (intrinsic and induced), so an accurate estimate of the upstream conditions is important to constraining the properties of Ganymede's internal magnetic field. In our study we focus on the upstream magnetic field conditions though the plasma conditions are also both temporally and spatially variable (e.g. Kivelson et al., 2022), which will affect the nature of the satellite-magnetosphere interaction (e.g. Bagenal and Dols, 2020).

This paper is organized as follows: section 2 reviews the availability of magnetic field measurements near Ganymede's orbit and the expected dependence on longitude. Section 3 summarizes the Galileo magnetic field measurements near Ganymede and their spatial (longitudinal and local time) and temporal variability. In section 4 we examine the magnetospheric conditions before and after Juno's orbit 34 Ganymede flyby, and we conclude with a summary in section 5.

## 2. Data availability and expected longitudinal dependence

Magnetic field measurements from Jupiter's magnetosphere are available from six spacecraft that flew through the system (Voyager 1, Voyager 2, Pioneer 10, Pioneer 11, Ulysses) and two orbiters (Galileo, 1996-2003; and Juno, 2016-present). Figure 1 shows the orbital coverage of all spacecraft that have visited the Jovian system except Cassini, which only briefly entered Jupiter's magnetosphere, and New Horizons, which did not carry a magnetometer. The spacecraft trajectories are shown in magnetospheric local time, System III latitude and longitude, and magnetic coordinates ("wiggle plot") as calculated using the JRM09 dipole tilt value of 10.31º toward 196.61º System III left-handed longitude (Connerney et al., 2018). Galileo's orbit was confined to near the jovigraphic equatorial plane, while Juno is in a polar 53-day orbit with an apoapsis of ~110 $R_J$ and an inclination that is increasing with time (Bolton et al., 2017). During the inbound portion of its initial orbits, Juno's latitude at ~10-20 $R_J$ was as large as ~20º but that latitude has decreased with time.

Ganymede orbits Jupiter in a nearly circular path (eccentricity = 0.001) with a semi-major axis 14.97 $R_J$ (1 $R_J$ = 71,492 km) and an orbital inclination of 0.18º. For simplicity, in our analysis we will take "Ganymede's orbit" to mean a circular path of radius 15 $R_J$ in Jupiter's jovigraphic equatorial plane. Most of the magnetic field measurements from the region near Ganymede's orbit come from Galileo, which completed over 30 orbits of Jupiter and collected magnetic field measurements with a typical time resolution of 24 seconds per vector. In just under half of its first 34 orbits, Juno passed through magnetic latitudes equivalent to the region near Ganymede's orbit, as shown in the bottom middle panel of Figure 1, though the spacecraft was typically located ~1 $R_J$ or more off the jovigraphic equator (see top right panel of Figure 1). Juno magnetic field measurements are available with a time resolution of 1 second per vector (Connerney et al., 2017). The other spacecraft that passed Ganymede's orbit (Pioneer 10, Pioneer 11, Voyager 1, Voyager 2, Ulysses) were typically located significantly off the jovigraphic equator, so we exclude them from our statistical analysis in the next section.

The magnetic field in Jupiter's innermost magnetosphere ($R$ < 10 $R_J$) is largely dipolar, while in the middle magnetosphere ($R$ > 30 $R_J$) the field becomes radially stretched by the currents flowing in the current sheet or plasma sheet. Outside of the Io plasma torus, the plasma in Jupiter's magnetosphere is concentrated in a plasma sheet that is roughly aligned with the magnetic equator inside of ~30 $R_J$ (Behannon et al., 1981). At Ganymede's orbit the magnetic equator and centrifugal equator, the point along each flux tube farthest from the planet, are nearly, but not exactly, aligned (Phipps and Bagenal, 2021). Jupiter's dipole field is tilted ~10º with respect to the planet's spin axis, toward ~200º west (left-handed) System III longitude. As a result, a spacecraft or moon near the jovigraphic equator – like Galileo and Ganymede – will observe the magnetic field fluctuating as its magnetic latitude oscillates from roughly +10º to -10º over the planet's ~10 hour rotation period. Therefore, both the magnitude and direction of the magnetic field upstream of Ganymede are strongly dependent on longitude. For example, the radial component of the magnetic field, $B_R$, reverses twice per planetary rotation as Jupiter's plasma sheet passes over the jovigraphic equator.

Figure 2, which we discuss further in the next section, shows the modeled longitudinal dependence of the magnetic field at Ganymede's orbit along with Galileo measurements from radial distances 14.95-15.05 $R_J$. A similar plot showing the longitudinal dependence of Juno data near Ganymede's orbit is given in Figure 3; we exclude Juno data from Figure 2 because most orbits are significantly off the jovigraphic equator and therefore are not representative of the magnetic field conditions near Ganymede. The model field, shown by the thick gray lines, is calculated using the JRM09 model for Jupiter's internal field plus the contribution of a current sheet from the Connerney et al. (2020) model ("CON2020") at a radial distance of 15 $R_J$ at the jovigraphic equator. This current sheet model is based on a Voyager-era model which represented

Jupiter's current sheet as an axisymmetric washer-shaped disk (Connerney et al., 1981). The Voyager-era model fit parameters are the inner and outer edge of the disk, the disk thickness, the current sheet azimuthal tilt, the azimuthal angle of the tilt, and the azimuthal current constant $\mu_0 I_0$, which represents the current sheet current density and is given in units of nT. The CON2020 model updated the original Voyager-era model by introducing a radial current constant $\mu_0 I_{rad}/2\pi$, also in units of nT, that produces a $B_\varphi$, the azimuthal component of the magnetic field, and controls the field bend back out of the meridian plane. Fitting the current constants to Galileo and Juno data on an orbit-by-orbit basis has provided a measurement of temporal activity in Jupiter's magnetosphere and can give insights into the expected field variability at Ganymede's orbit (Vogt et al., 2017; Connerney et al., 2020). Finally, we note that other external field models (e.g. Khurana, 1997) predict similar magnetic field conditions near Ganymede's orbit, as shown in Figure S1.

## 3. Galileo magnetic field observations near Ganymede: spatial and temporal variability

The measurements and model predictions plotted in Figure 2 provide an overview of the typical magnetic field conditions upstream of Ganymede and their spatial and temporal variability. The figure shows the three field components in System III spherical coordinates, the magnetic field bendback and elevation angles, and the field magnitude as a function of longitude. The magnetic field bendback angle $\alpha$ indicates the angle of the magnetic field out of a meridian plane and is defined by $\alpha = \tan^{-1}\left(\frac{B_\varphi}{B_R}\right)$ so that a negative (positive) bendback angle indicates a swept back (swept forward) field configuration. The field elevation angle, $\theta_{elevation}$, indicates the angle that the magnetic field makes with respect to the radial direction in the $R$-$\theta$ plane and is defined by $\theta_{elevation} = \tan^{-1}\left(\frac{-B_\theta}{|B_R|}\right)$ so that the elevation angle is positive for a southward field and is 90º when the field is completely southward. We evaluate both angles only when $|B_R| > 3$ nT because small fluctuations in $B_R$ can lead to large fluctuations in the field angles when $B_R$ is small. Figure 2 includes all Galileo measurements from radial distances 14.95-15.05 $R_J$ and all latitudes, excepting the six close flybys of Ganymede when the spacecraft was measuring Ganymede's magnetospheric field.

The data and model predictions in Figure 2 show overall good agreement and can be used together to characterize the magnetic field conditions near Ganymede's orbit, which we summarize in Table 1. The average $|B|$ value near Ganymede is ~95-100 nT according to both the data and model, and the field is typically oriented mostly in the north-south direction and only weakly swept out of the meridian plane (the model predicts $|B_\theta| > |B_R|$ and $|\alpha| < 20°$ at roughly 70 percent of longitudes). The magnetic field orientation is therefore generally favorable for reconnection at Ganymede's magnetopause since the satellite's internal magnetic field is oriented almost completely northward, with a dipole tilt of 176º from its spin axis (Kivelson et al., 2002; Kaweeyanun et al., 2020).

The field near Ganymede's orbit changes on time scales that are longer than the ~10 hour planetary rotation period, as shown by orbit-to-orbit changes in the observed field values plotted in Figure 2. Some of the orbit-to-orbit variation may be accounted for by the orbits' spatial, not temporal, differences. For example, the magnetic field and plasma properties in Jupiter's magnetosphere vary with local time (e.g. Palmaerts et al., 2017 and references therein) so that $B_\theta$ near Ganymede's orbit will vary by ~9 nT (~10%) over the satellite's ~7 day orbital period, as shown in Figure S2. The $B_\theta$ local time dependence can also be seen in Figure 2, as $B_\theta$ measurements collected at local times near 15:00 (purple and dark blue) are generally larger than those collected at local times far from 15:00 (green and red). However, most of the orbit-to-orbit variability in the magnetic field indicates variable magnetospheric conditions due to activity like magnetospheric injections, mass loading due to volcanic activity on Io, or even changes in the external solar wind conditions (e.g. Mauk et al., 1999; Louarn et al., 2014; Tao et al., 2005; Vogt et al., 2019).

In general, the magnitude of these orbit-by-orbit temporal changes is significantly smaller than the magnitude of the variations with longitude. For example, the two dashed gray lines in Figure 2 show the expected range of the JRM09 + CON2020 modeled field conditions. To calculate these maximum and minimum model values we used the range of best fit current constants fit to individual Juno orbits listed in Table 2 of Connerney et al. (2020). The average temporal change in $|B|$ expected from the current sheet variability is ~5 nT, but it can be as large as ~12 nT near the magnetic equator. The modeled differences in the individual field components, which we list in Table 1, typically represent a ~10-20 percent variability in the baseline values (note that the change in $B_R$ and $B_\varphi$ depends strongly on longitude). Figure S3 illustrates how changes in the CON2020 current constants affect the predicted individual field components near Ganymede's orbit. In general, changes to the radial current constant $I_\rho$ have only a very small effect on $B_R$ and $B_\theta$ but can significantly influence $B_\varphi$, particularly at high magnetic latitudes (near the longitude of the dipole tilt and 180º away from it). Near the magnetic equator only $B_\theta$ is strongly dependent on $\mu_0 I_0$.

Finally, in Figure 3 we show the values of the magnetic field measured by Galileo in the general vicinity of Ganymede, organized by position in magnetic cylindrical coordinates. Each panel is divided into boxes spanning 0.05 $R_J$ in $\rho_{mag}$ (cylindrical radial distance) by 0.25 $R_J$ in $z_{mag}$, with color indicating quantities like the average or standard deviation of the measured magnetic field in each box. This figure gives insight into the expected field variability at Ganymede's orbit on both short (~10 hour) and long (orbit-by-orbit) time scales. The average $B_R$ is very well-organized by magnetic coordinates, indicating that the $B_R$ near Ganymede is relatively constant on long time scales (weeks to months) but varies strongly as Ganymede's position in magnetic coordinates (pink curves in Figure 3) change over a planetary rotation period. By comparison, the plot of the average $B_\varphi$ is extremely disorganized, indicating that it is highly variable on long time scales.

Figure 3 also shows that the long-term temporal variability of $B_R$ and $B_\theta$, as indicated by the standard deviation plots, is typically ~ a few nT, which is roughly consistent with the CON2020 modeled temporal variability. This can also be seen in Figure 2, where the magnitude of the scatter in $B_R$ and $B_\theta$ at a given longitude is roughly consistent with the modeled current sheet variability (the difference between the two dashed gray lines) but the scatter in the measured $B_\varphi$ is significantly larger than the temporal variability predicted by the CON2020 model. Analogous plots made using Juno data are provided in Figure S4, though we note that each colored box typically contains data from only one Juno orbit because of the limited data coverage at low jovigraphic latitudes. Therefore, the standard deviations plotted in Figure S4, are typically smaller for Juno than for Galileo because they indicate temporal variability on short (seconds or minutes) timescales rather than orbit-to-orbit variability.

## 4. Magnetospheric conditions at the time of Juno's Ganymede flyby

Juno's close Ganymede flyby occurred on 7 June 2021, with closest approach at 16:56 UT at a subspacecraft SIII right handed longitude of 57.5º (Hansen et al., this issue). The spacecraft encountered Ganymede's magnetosphere and wake at SIII right handed longitudes ~70º to ~50º, when Ganymede was just south of the magnetic equator and very close to the center of the plasma sheet. (A radial distance of 15 $R_J$ at the jovigraphic equator and SIII longitudes 50º to 70º corresponds to magnetic latitudes of -2.5º to 0.7º and $z_{mag}$ from -0.66 $R_J$ to 0.18 $R_J$.) We follow three steps in estimating the magnetic field conditions upstream of Ganymede.

First, we consider the predicted conditions using the JRM09 + CON2020 average and temporally varying model. The JRM09 + CON2020 model (with average current constant values) predicts the following field values for SIII longitudes 50º-70º (see Table 2): $B_R$ ~ -29 nT to ~0 nT, $B_\theta$ ~ 69 nT, $B_\varphi$ ~ -10 nT to -13 nT, $|B|$ ~ 76 nT to 71 nT, bendback angle ~ 20º-85º, and elevation angle ~ 70º-89º. At those longitudes, using the largest or smallest best fit values of the CON2020 current constants rather than the average values would change the modeled field components roughly as follows: $B_R$ ±1 nT, $B_\theta$ ± 6 nT, $B_\varphi$ ±1 nT, $|B|$ ± 5 nT. This gives us the full range of expected field conditions at the time of Juno's Ganymede flyby and shows that the individual field components and field magnitude can vary by as much as ±5-10 percent of their average values.

Second, we fit the data to the CON2020 model to obtain a rough estimate of the best fit current constants to evaluate the state of the magnetosphere during orbit 34. We followed Vogt et al. (2017) in varying only the $\mu_0 I_0$ parameter to fit $B_\theta$, at radial distances 10 to 30 $R_J$ during each orbit's inbound pass and excluding the Ganymede flyby interval during orbit 34. We then fit the measured $B_\varphi$ by varying the radial current constant value with the best fit $\mu_0 I_0$ calculated for each orbit. For both $\mu_0 I_0$ and $\mu_0 I_{rad}/2\pi$ we estimated the best fit by calculating the model field at a range of values (with a 2 nT step size) and minimizing the root mean square error between the external (measured – JRM09 internal field) and model field. Though our approach differs slightly from Connerney et al. (2020) we obtained nearly identical best fit $\mu_0 I_0$ values for Juno's first 24 orbits (see Figure S5), which gives us confidence in the validity of our fits estimates. We found that the first 34 Juno orbits featured an average $\frac{\mu_0 I_0}{2}$ fit of 144.3 nT (standard deviation 8.5 nT), consistent with the average 140.2 nT Connerney et al. (2020) reported from Juno's first 24 orbits.

For orbit 34 we calculated a best fit $\frac{\mu_0 I_0}{2}$ fit of 138 nT, slightly below average. Our calculated best fit $\mu_0 I_{rad}/2\pi$ was 44 nT, though we note that the goodness of the $B_\varphi$ fit was nearly independent of the radial current constant in orbit 34 and that our fit approach closely reproduced the Connerney et al. (2020) $\mu_0 I_0$ fit value but not the $\mu_0 I_{rad}/2\pi$ (our average was 23.8 nT, compared to 16.7 nT from Connerney et al. (2020); see Figure S6).

Finally, we compare the field measured by Juno during orbit 34 to the Galileo average along Juno's trajectory in magnetic coordinates, as shown in Figure 5. The black lines show Juno orbit 34 data as a function of $\rho_{mag}$, while the red lines in each panel show the Galileo average magnetic field values in each ($\rho_{mag}$, $z_{mag}$) bin from Figure 4 along Juno's trajectory (thick white line in Figure 4), and error bars show the standard deviation within the bins. This comparison shows that the magnetic field conditions in Jupiter's magnetosphere immediately before and after Juno's close Ganymede flyby were, overall, within the range of the typical Galileo measurements. The Juno field magnitude is typically slightly smaller than the Galileo averages, due in part to differences in $B_\varphi$, which is highly variable in this area. However, the Juno $B_\theta$ values are also systematically slightly smaller than the Galileo averages, which is consistent with Connerney et al. (2020)'s finding that the Juno-era height-integrated current in the magnetodisk is ~15% smaller than in the Pioneer, Voyager, and Galileo eras.

Overall, we find that the magnetic field measurements near Ganymede's orbit from Juno orbit 34 are well-described by the JRM09 internal field plus the *average* CON2020 model external field (blue lines in Figure 5). Only the $B_\varphi$ component is systematically poorly fit by both the average Galileo field and by the JRM09+CON2020 model; the model field predicts $B_\varphi$ ~ -11 nT at Ganymede though the observed $B_\varphi$ is ~ -14 nT. The average model would therefore provide a good estimate of Jupiter's magnetospheric field during the flyby, though a better fit would use the slightly modified current constant parameters and would manually adjust the $B_\varphi$ fit. Overall, the measured $|B|$ near Ganymede's orbit during Juno orbit 34 differs from the average JRM09+CON2020 model $|B|$ by only about ~2 percent and there is no systematic offset in $|B|$ or in $B_\theta$ as one would expect if the magnetodisk currents were significantly different from their average values.

**5. Conclusions and Summary**

The magnetic field conditions upstream of Ganymede display both spatial and temporal variability that can influence the moon-magnetosphere interaction. The spatial variability includes a local time dependence and, most significantly, a dependence on longitude due to Jupiter's ~10º dipole tilt. The longitudinal dependence is significantly larger than the observed orbit-to-orbit variability, with $|B|$ fluctuating from ~65 to ~125 nT during each planetary rotation. The field direction also varies significantly, with the bendback angle ranging from roughly -85º (almost completely swept back) to +85º (almost completely swept forward) and the elevation angle ranging from ~35º to ~90º (completely southward).

Galileo data from near the jovigraphic equator show that the longitudinal dependence of the magnetic field near Ganymede's orbit is well-described by the combined JRM09 internal field model (Connerney et al., 2018) and CON2020 external field model (Connerney et al., 2020), which computes the field due to Jupiter's current sheet. The CON2020 model includes azimuthal and radial current constant parameters that can be fit to data from each Galileo or Juno orbit to obtain a measure of the variability in Jupiter's magnetodisk. The expected orbit-to-orbit temporal variability obtained from these current sheet fits represents a ~10-20 percent variability in the baseline values of the individual field components and $|B|$, though the exact details depend on longitude. This possible variability should be considered when making preparations, such as reanalysis of Galileo flyby data or modeling work, for the upcoming NASA Europa Clipper and ESA JUICE missions.

During orbit 34, Juno flew past Ganymede at SIII right handed longitudes ~70º to ~50º, when Ganymede was just south of the magnetic equator and very close to the center of the plasma sheet. At these longitudes the expected average field conditions based on the JRM09+CON2020 model would be: $B_R$ ~ -29 nT to ~0 nT, $B_\theta$ ~ 69 nT, $B_\varphi$ ~ -10 nT to -13 nT, $|B|$ ~ 76 nT to 71 nT, bendback angle ~ 20º-85º, and elevation angle ~ 70º-89º. We calculated the best fit current constant parameters to Juno magnetic field data from orbit 34 and also compared the magnetic field along Juno's trajectory to Galileo averages from the same positions in magnetic coordinates. Our analysis showed that Jupiter's magnetospheric field during orbit 34 was very close to its average state. Overall, the orbit 34 data near Ganymede's orbit are well-described by the JRM09+CON2020 average model, with only the $B_\varphi$ component being systematically underestimated (predicted -11 nT compared to -14 nT observed). We look forward to future Juno, Europa Clipper, and JUICE data from Jupiter's inner magnetosphere that should provide new insight into the nature and causes of the temporal variability in Jupiter's magnetodisk and its influence on the plasma environments of the Galilean satellites.

**Acknowledgements**

We gratefully acknowledge helpful discussions with Jack Connerney. The JRM09 + CAN2020 current sheet code used to create several figures was developed by M.F.V. in collaboration with Rob Wilson, Gabby Provan, Matt James, and Marty Brennan and is available at https://github.com/marissav06/jovian_jrm09_internal and https://github.com/marissav06/con2020_idl. Magnetometer data from all spacecraft that have visited the Jovian system are available from the Planetary Data System. Specifically, Galileo data can be downloaded from https://pds-ppi.igpp.ucla.edu/search/?sc=Galileo&t=Jupiter&i=MAG, and Juno data can be downloaded from https://pds-ppi.igpp.ucla.edu/search/?sc=Juno&t=Jupiter&i=FGM. M.F.V. was supported by NASA grant 80NSSC20K0559 and by the Juno Participating Scientist program.

## References


Bagenal, F., & Dols, V. (2020). The space environment of Io and Europa. Journal of Geophysical Research: Space Physics, 125, e2019JA027485. https://doi.org/10.1029/2019JA027485

Behannon, K. W., L. F. Burlaga, and N. F. Ness (1981), The Jovian magnetotail and its current sheet, *J. Geophys. Res.*, *86*, 8385-8401.

Bolton, S.J., Lunine, J., Stevenson, D. et al. Space Sci Rev (2017) 213: 5. https://doi.org/10.1007/s11214-017-0429-6

Connerney, J., M. Acuña, and N. Ness (1981), Modeling the Jovian Current Sheet and Inner Magnetosphere, *J. Geophys. Res.*, *86*(A10), 8370-8384.

Connerney, J.E.P., Benn, M., Bjarno, J.B., Denver, T., Espley, J., Jorgensen, J.L., et al. (2017). The Juno magnetic field investigation, Space Sci. Rev., 213(1-4), 39-138, doi: 10.1007/s11214-017-0334-z.

Connerney, J. E. P., Kotsiaros, S., Oliversen, R. J., Espley, J. R., Joergensen, J. L., Joergensen, P. S., et al. (2018). A new model of Jupiter's magnetic field from Juno's first nine orbits. Geophysical Research Letters, 45. https://doi.org/10.1002/2018GL077312

Connerney, J. E. P., Timmins, S., Herceg, M., & Joergensen, J. L. (2020). A Jovian magnetodisc model for the Juno era. *Journal of Geophysical Research: Space Physics*, *125*, e2020JA028138. https://doi.org/10.1029/2020JA028138

Hansen, C. J, et al., Juno's Close Encounter with Ganymede – an Overview, submitted to Geophys. Res. Lett., this issue.

Jia, X., Walker, R. J., Kivelson, M. G., Khurana, K. K., and Linker, J. A. (2009), Properties of Ganymede's magnetosphere inferred from improved three-dimensional MHD simulations, J. Geophys. Res., 114, A09209, doi:10.1029/2009JA014375.

Jia, X., Walker, R. J., Kivelson, M. G., Khurana, K. K., and Linker, J. A. (2010), Dynamics of Ganymede's magnetopause: Intermittent reconnection under steady external conditions, J. Geophys. Res., 115, A12202, doi:10.1029/2010JA015771.

Kaweeyanun, N., Masters, A., & Jia, X. (2020). Favorable conditions for magnetic reconnection at Ganymede's upstream magnetopause. Geophysical Research Letters, 47, e2019GL086228. https://doi.org/10.1029/2019GL086228

Khurana, K. K. (1997), Euler potential models of Jupiter's magnetospheric field, *J. Geophys. Res.*, *102*(A6), 11295-11306.

Kivelson, M. G., K. K. Khurana, C. T. Russell, R. J. Walker, J. Warnecke, F. V. Coroniti, C. Polanskey, D. J. Southwood, and G. Schubert (1996), Discovery of Ganymede's magnetic field by the Galileo spacecraft, *Nature, 384,* 537 - 541.

Kivelson, M. G., Khurana, K. K., Stevenson, D. J., Bennett, L., Joy, S., Russell, C. T., Walker, R. J., Zimmer, C., and Polanskey, C. (1999), Europa and Callisto: Induced or intrinsic fields in a periodically varying plasma environment, J. Geophys. Res., 104( A3), 4609– 4625, doi:10.1029/1998JA900095.

Kivelson, M.G., Khurana, K. K., & Volwerk, M. (2002), The permanent and inductive magnetic moments of Ganymede, Icarus, 157, 507–522, doi:10.1006/icar.2002.6834.

Kivelson, M. G. et al., “Ganymede: Its Magnetosphere and its Interaction with the Jovian Magnetosphere”, in: “Ganymede”, eds. M. Volwerk, M. McGrath, X. Jia and T. Spohn, Cambridge University Press, Cambridge, UK,  pre-press, 2022.

Louarn, P., C. P. Paranicas, and W. S. Kurth (2014), Global magnetodisk disturbances and energetic particle injections at Jupiter, *J. Geophys. Res. Space Physics*, *119*, 4495–4511, doi:10.1002/2014JA019846.

Mauk, B. H., D. J. Williams, R. W. McEntire, K. K. Khurana, and J. G. Roederer (1999), Storm-like dynamics of Jupiter's inner magnetosphere, *J. Geophys. Res*., *104*, 22,759.

Palmaerts, B., Vogt, M. F., Krupp, N. , Grodent, D. and Bonfond, B. (2017). Dawn-Dusk Asymmetries in Jupiter's Magnetosphere. In Dawn-Dusk Asymmetries in Planetary Plasma Environments (eds S. Haaland, A. Runov and C. Forsyth). doi:10.1002/9781119216346.ch24

Phipps, P., & Bagenal, F. (2021). Centrifugal equator in Jupiter's plasma sheet. Journal of Geophysical Research: Space Physics, 126, e2020JA028713., DOI: https://doi.org/10.1029/2020JA028713

Russell, C. T., Z. J. Yu, K. K. Khurana, and M. G. Kivelson (2001), Magnetic field changes in the inner magnetosphere of Jupiter, *Adv. Space Res.*, *28*(6), 897-902.

Tao, C., R. Kataoka, H. Fukunishi, Y. Takahashi, and T. Yokoyama (2005), Magnetic field variations in the Jovian magnetotail induced by solar wind dynamic pressure enhancements, *J. Geophys. Res.*, *110*, A11208, doi:10.1029/2004JA010959.

Tóth, G., Jia, X., Markidis, S., Peng, I. B., Chen, Y., Daldorff, L. K. S., Tenishev, V. M., Borovikov, D., Haiducek, J. D., Gombosi, T. I., et al. (2016), Extended magnetohydrodynamics with embedded particle-in-cell simulation of Ganymede's magnetosphere, J. Geophys. Res. Space Physics, 121, 1273– 1293, doi:10.1002/2015JA021997.

Vogt, M. F., E. J. Bunce, J. D. Nichols, J. T. Clarke, and W. S. Kurth (2017), Long-term variability of Jupiter's magnetodisk and implications for the aurora, Journal of Geophysical Research: Space Physics, 122, 12,090–12,110, doi:10.1002/2017JA024066.

Vogt, M. F., Gyalay, S., Kronberg, E. A., Bunce, E. J., Kurth, W. S., Zieger, B., & Tao, C. (2019). Solar wind interaction with Jupiter's magnetosphere: A statistical study of Galileo in situ data and modeled upstream solar wind conditions. Journal of Geophysical Research: Space Physics, 124, 10170– 10199. https://doi.org/10.1029/2019JA026950

Zhou, H., Tóth, G., Jia, X., & Chen, Y. (2020). Reconnection-driven dynamics at Ganymede's upstream magnetosphere: 3-D global Hall MHD and MHD-EPIC simulations. Journal of Geophysical Research: Space Physics, 125, e2020JA028162. https://doi.org/10.1029/2020JA028162

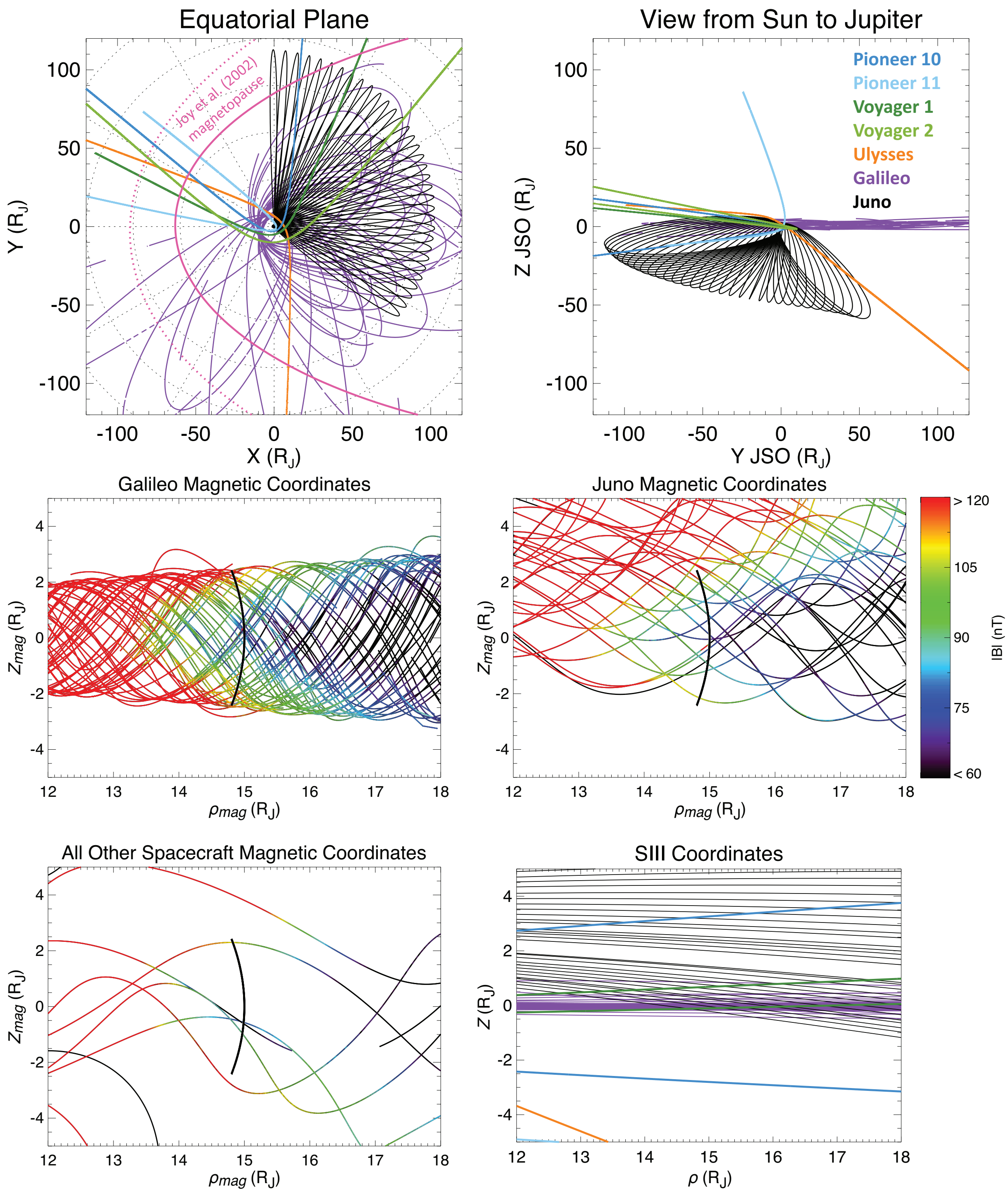


**Figure 1.** Trajectories of all spacecraft that have visited Jupiter's magnetosphere except Cassini and New Horizons. Top left: spacecraft trajectories projected onto the equatorial plane, with the Joy et al. (2002) magnetopause boundaries in pink. Top right: spacecraft trajectories as viewed

from the sun in JSO coordinates. Middle left: “wiggle plot” showing Galileo’s orbital coverage near Ganymede’s orbit, plotted in JRM09 magnetic cylindrical coordinates with color indicating the measured magnetic field magnitude. The thick black line shows the possible range of Ganymede’s location (15 $R_J$ radial distance and 0º jovigraphic latitude). Middle right: “wiggle plot” showing Juno’s orbital coverage near Ganymede’s orbit, plotted in JRM09 magnetic cylindrical coordinates. Bottom left: “wiggle plot” showing trajectories of Pioneers 10 and 11, Voyagers 1 and 2, and Ulysses near Ganymede’s orbit, plotted in JRM09 magnetic cylindrical coordinates. Bottom right: spacecraft trajectories in System III cylindrical coordinates near Ganymede’s orbit.

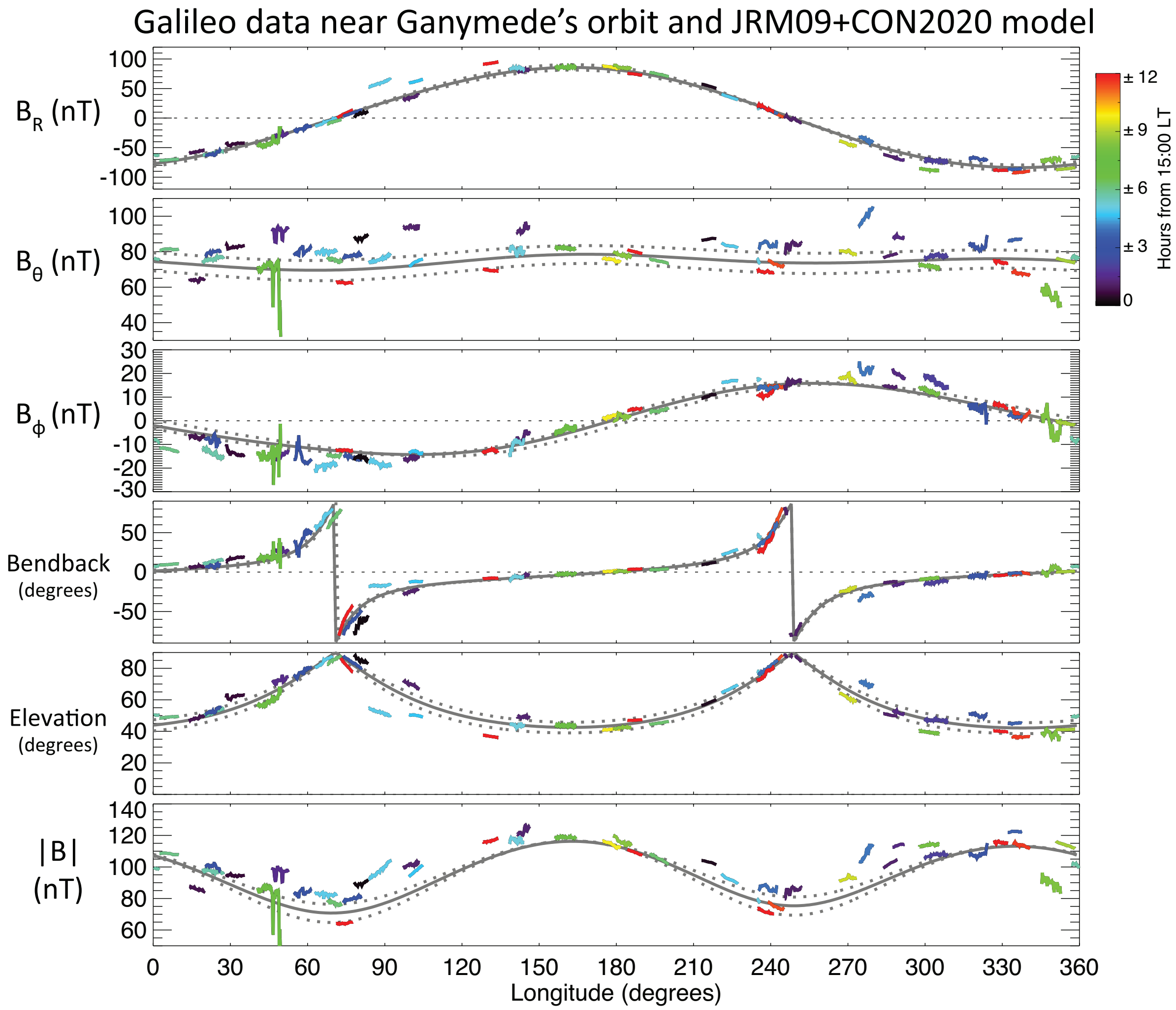


**Figure 2.** Dependence of the magnetic field near Ganymede's orbit as a function of System III right-handed longitude, as measured by Galileo at radial distances 14.95-15.05 $R_J$, excluding the spacecraft's six close flybys of Ganymede. From top: the radial ($B_R$), meridional ($B_\theta$), and azimuthal ($B_\varphi$) components of the magnetic field in nT, the field bendback and elevation angles in degrees, and the field magnitude ($|B|$) in nT. Color indicates the number of hours of local time from 15:00. Gray solid lines show the field predicted by the average JRM09 + CON2020 model (Connerney et al., 2018, 2020) at Ganymede's orbit while the dashed lines show the range of the expected field conditions based on model fits to individual Juno orbits (Connerney et al., 2020).

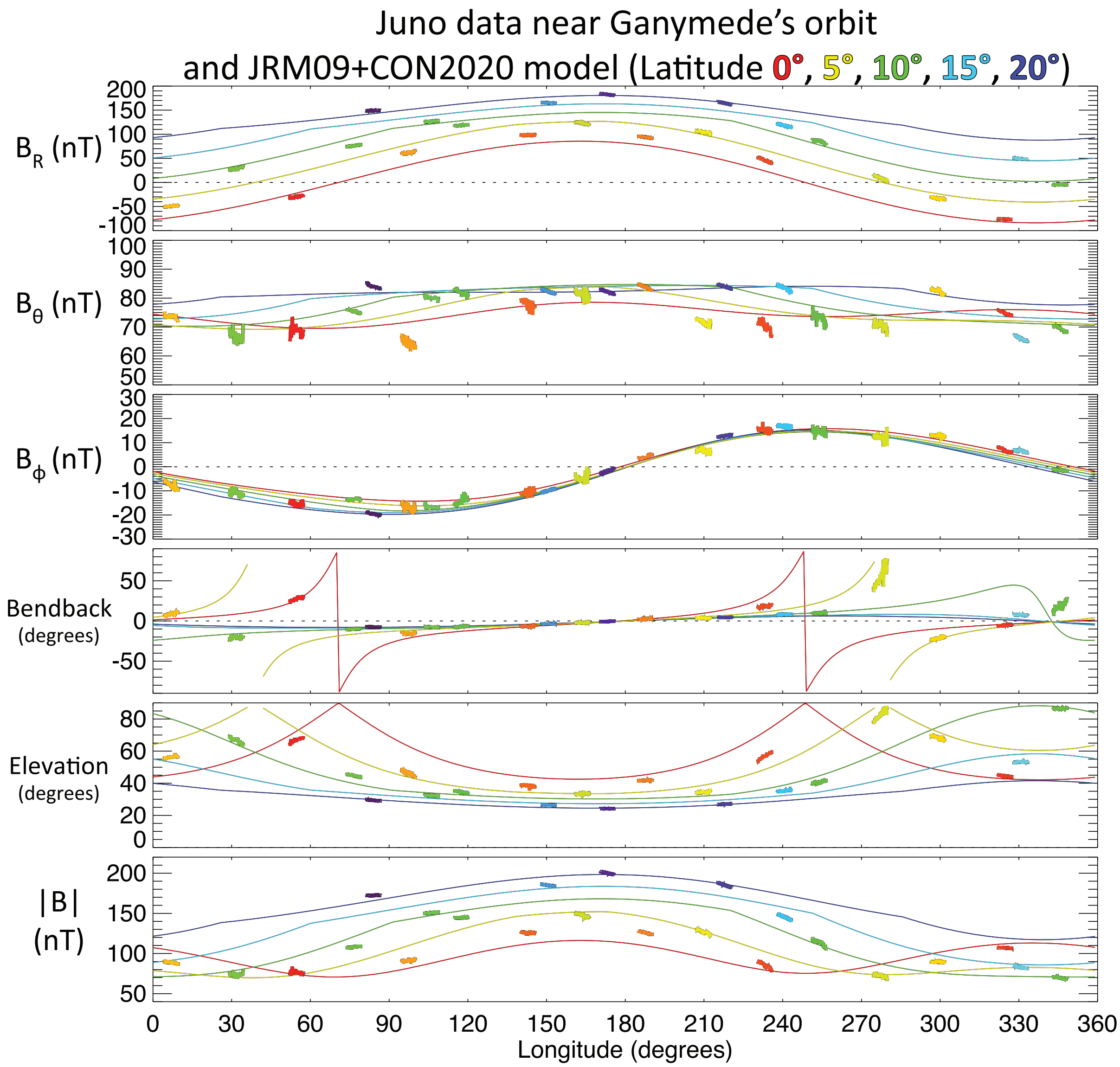


**Figure 3.** Dependence of the magnetic field near Ganymede's orbit as a function of System III right-handed longitude, from Juno's first 33 orbits at radial distances 14.95-15.05 $R_J$. From top: the radial ($B_R$), meridional ($B_\theta$), and azimuthal ($B_\varphi$) components of the magnetic field in nT, the field bendback and elevation angles in degrees, and the field magnitude $|B|$ in nT. The red solid line in each panel shows the quantity predicted by the JRM09 + CON2020 model (Connerney et al., 2018, 2020) at 15 $R_J$ at the jovigraphic equator, while other colored lines show the model predictions at 5º, 10º, 15º, and 20º jovigraphic latitude as noted.

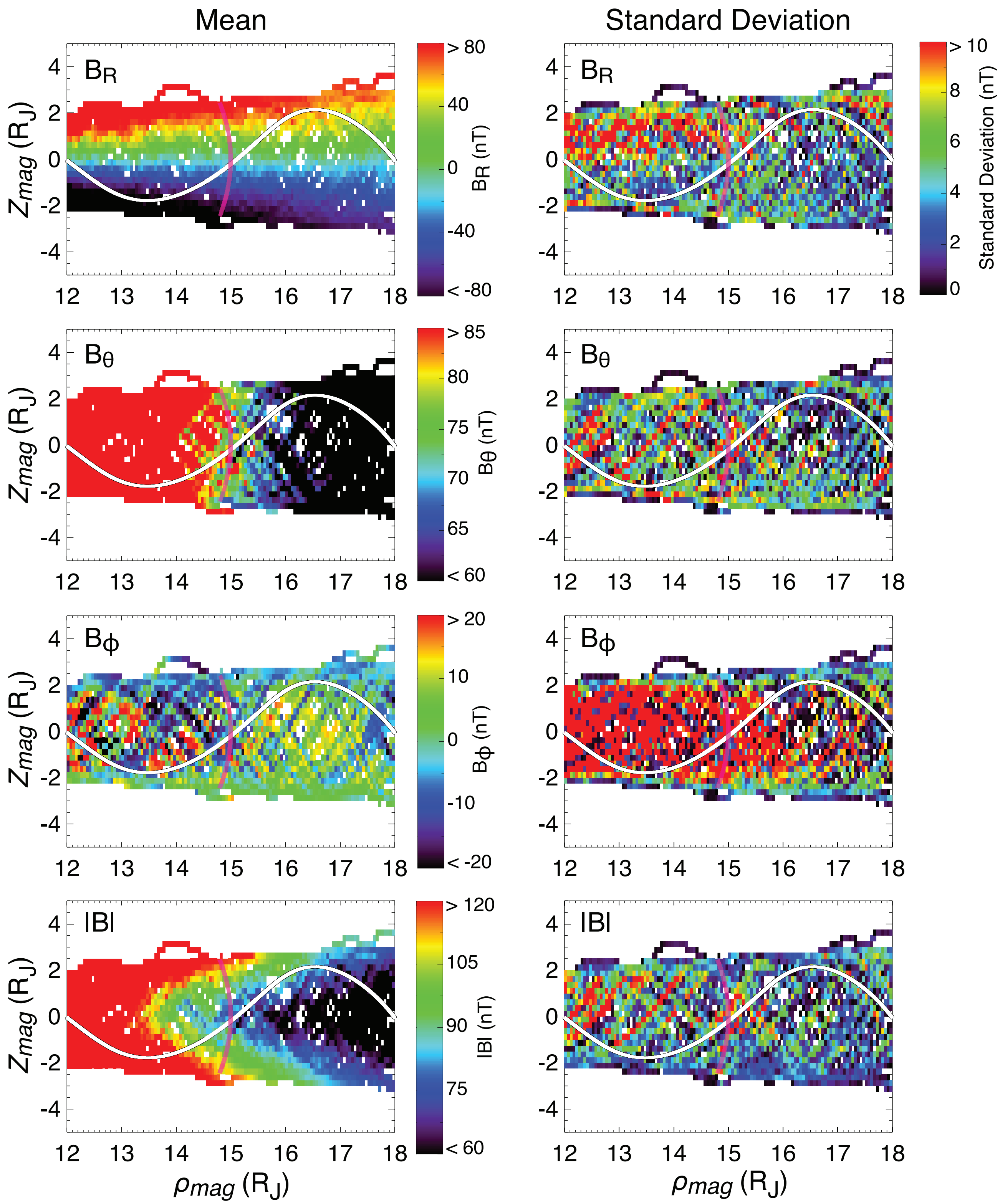


**Figure 4.** Magnetic field conditions measured by Galileo near Ganymede's orbit, organized in magnetic cylindrical coordinates. Boxes spanning 0.05 $R_J$ in $\rho_{mag}$ by 0.25 $R_J$ in $z_{mag}$ are drawn with

the color of each box indicating the mean measured magnetic field (left column) or standard deviation of the measured magnetic field (right column) in each box. Thick white lines in each panel show Juno's trajectory during orbit 34 and pink curves show the range of Ganymede's possible positions.

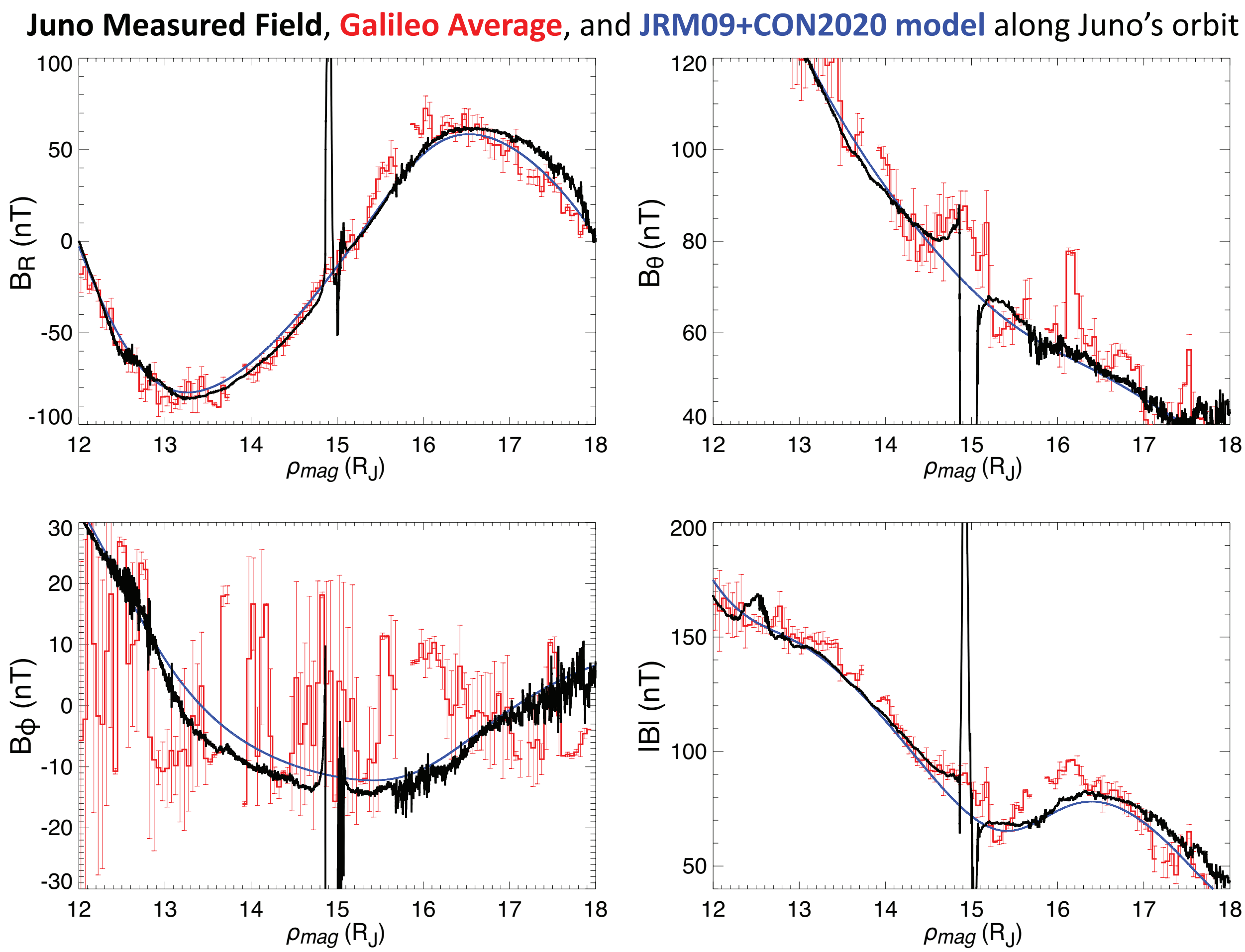


**Figure 5.** Magnetic field components and magnitude measured by Juno during orbit 34 as a function of magnetic cylindrical distance $\rho_{mag}$. Also shown in red are the average magnetic field measured by Galileo, with error bars indicating the standard deviation, along Juno's trajectory in magnetic coordinates, calculated in bins of 0.05 $R_J$ in $\rho_{mag}$ and 0.25 $R_J$ in $z_{mag}$. Blue lines show the JRM09+CON2020 model field.

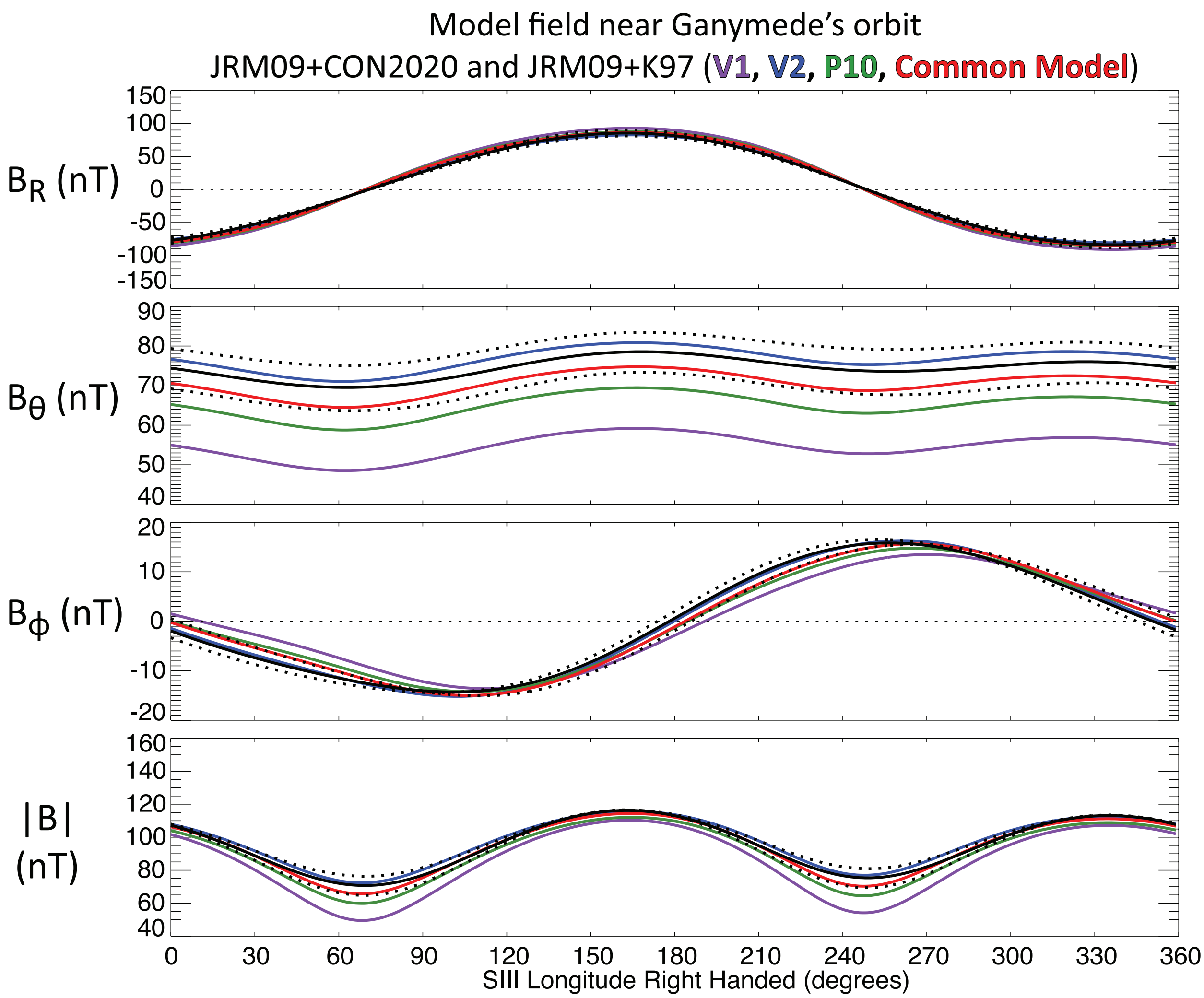


**Figure S1.** Dependence of the JRM09 internal field model and the Khurana (1997) modeled external magnetic field ("JRM09+K97") near Ganymede's orbit as a function of longitude. Colored lines show the model as fit to magnetic field data from Voyager 1 (purple), Voyager 2 (blue), Pioneer 10 (green), and the "common model" (red). Black lines show the average JRM09 + CON2020 model field, with dashed lines showing the range of the expected field conditions based on model fits to individual Juno orbits (Connerney et al., 2020). The two models predict broadly similar field values and longitudinal dependence, particularly for JRM09+K97 with Voyager 2 and common model parameters.

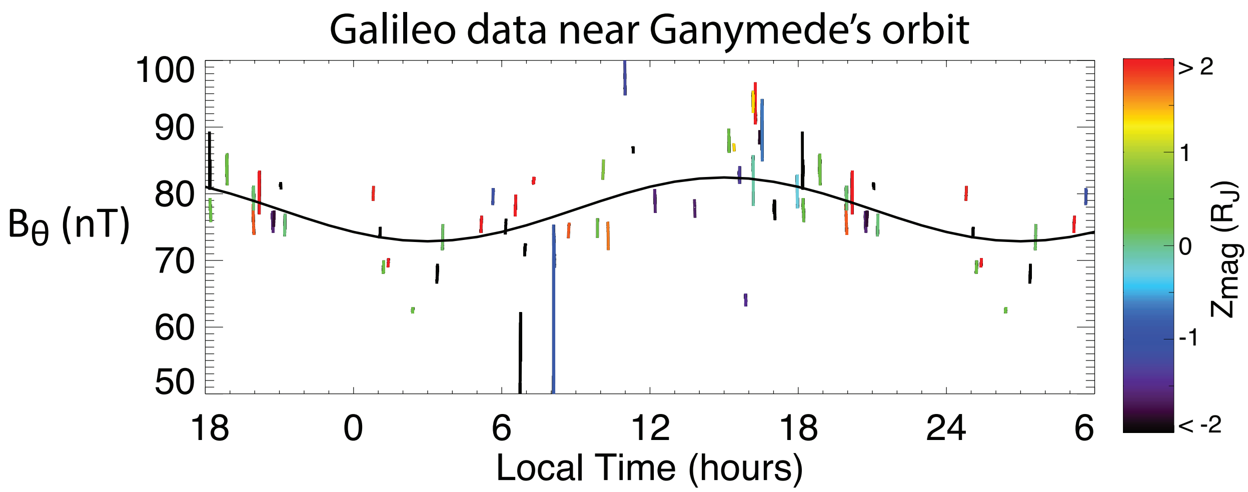


**Figure S2.** Local time dependence of $B_\theta$ measured by Galileo near Ganymede's orbit. Plotted are all available data (all local times and longitudes) except Galileo's six close Ganymede encounters. Colors indicate $z_{mag}$, the height from the magnetic equatorial plane in magnetic cylindrical coordinates. The thick black line shows the JRM09 + CON2020 model field averaged over all longitudes plus an external field local time variability fit calculated by Vogt et al. (2017).

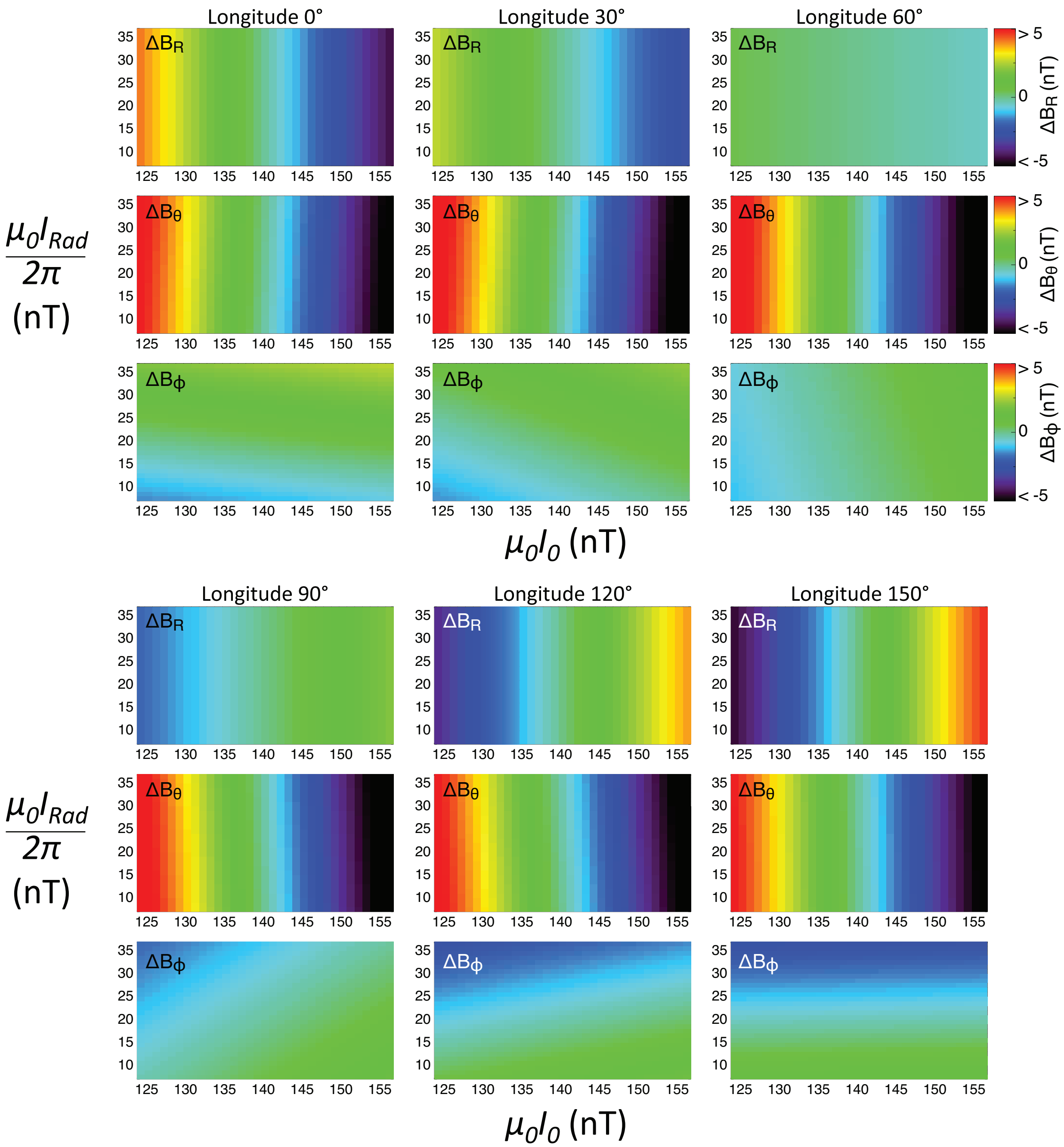


**Figure S3.** Dependence of the magnetic field produced by the CON2020 current sheet model on different values of the azimuthal current constant $\mu_0 I_0$ and the radial current constant $\mu_0 I_{rad}/2\pi$. For each $\mu_0 I_0$ and $\mu_0 I_{rad}/2\pi$ value the color plotted indicates the difference $(\Delta B_R, \Delta B_\theta, \Delta B_\varphi)$ between the model output using those current constants and the “average” model output using the CON2020 generic current constant values from fits to Juno data ($\mu_0 I_0$=139.6 nT, $\mu_0 I_{rad}/2\pi$ =

16.7 nT). All other current sheet parameters remain the same. Results are calculated at 15 $R_J$ at the jovigraphic equator and are shown for longitudes 0º to 150º System III right handed in 30º increments. The nearly vertical color bands in the $\Delta B_\theta$ panels at all longitudes show that $B_\theta$ is strongly dependent on $\mu_0 I_0$ but not on $\mu_0 I_{rad}/2\pi$. Similarly, at some longitudes (0º, 150º, which are the longitudes when Ganymede is at its highest magnetic latitude) $\Delta B_R$ is strongly dependent on $\mu_0 I_0$ but not on $\mu_0 I_{rad}/2\pi$, though at other longitudes $\Delta B_R$ is nearly independent of both current constants. At high magnetic latitudes, $\Delta B_\varphi$ is most strongly independent on $\mu_0 I_{rad}/2\pi$.

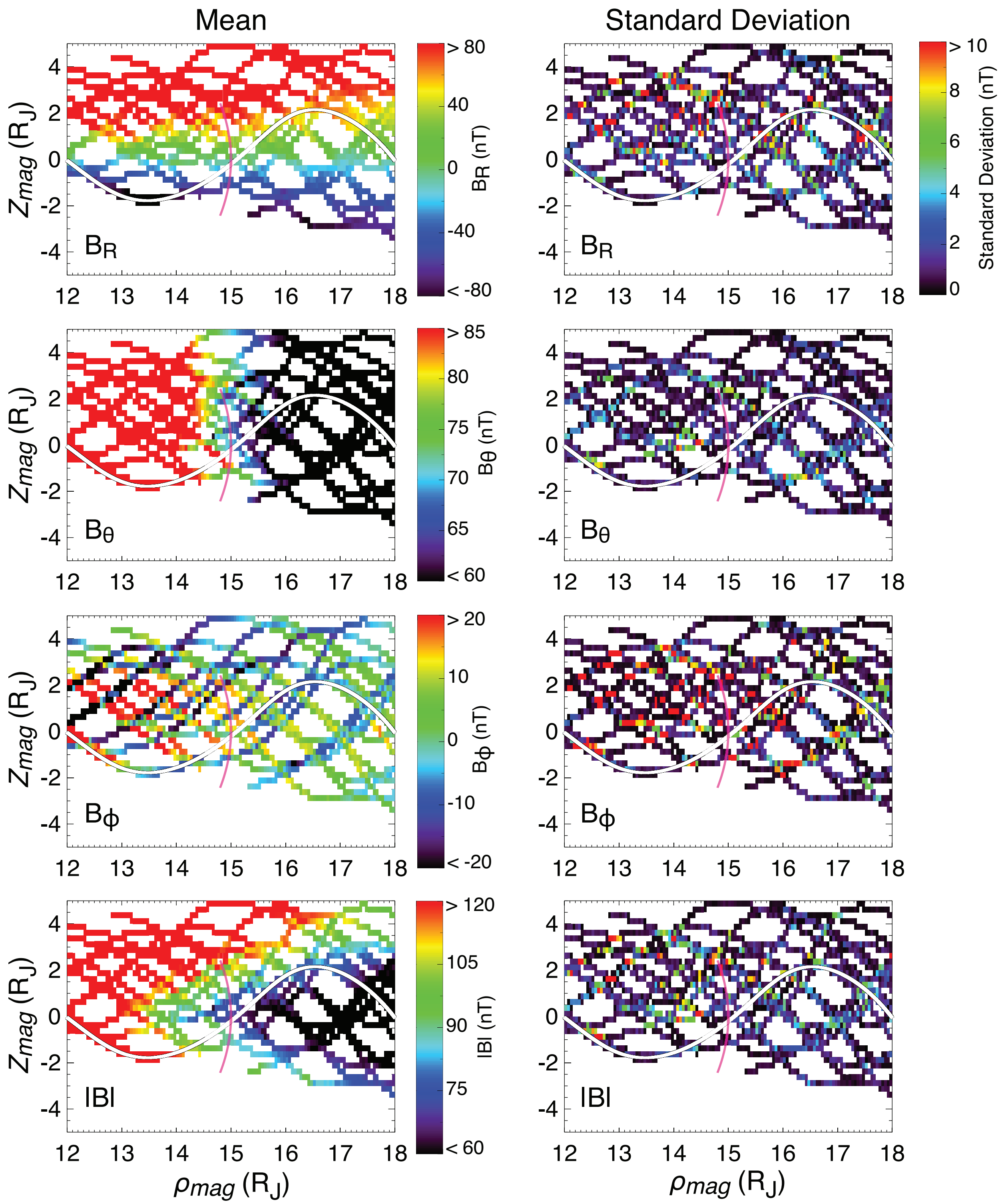


**Figure S4.** Magnetic field conditions measured by Juno near Ganymede's orbit, organized in magnetic cylindrical coordinates. Boxes spanning 0.05 $R_J$ in $\rho_{mag}$ by 0.25 $R_J$ in $z_{mag}$ are drawn with the color of each box indicating the mean (left column) or standard deviation (right column) of the measured magnetic field in each box. Thick white lines in each panel show Juno's trajectory during orbit 34 and pink curves show the range of Ganymede's possible positions.

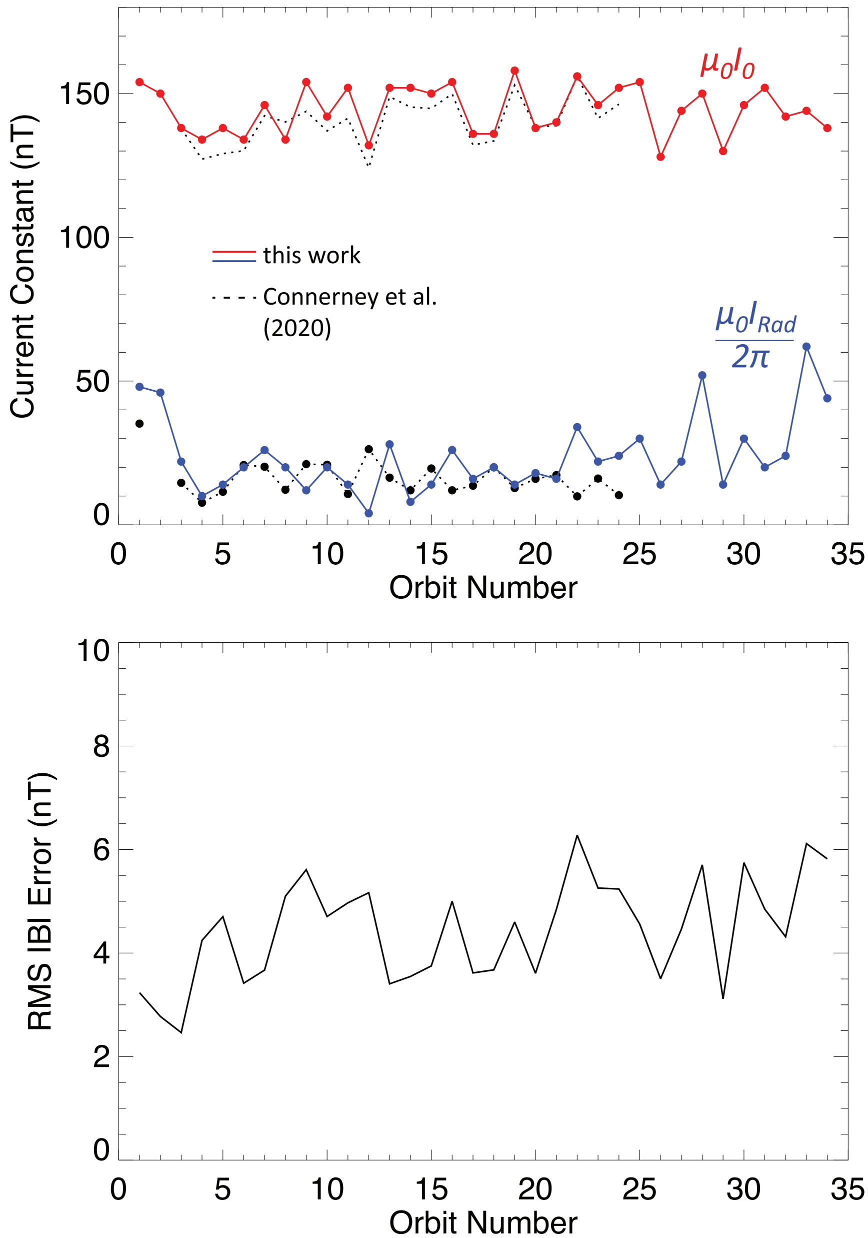


**Figure S5.** (top) Best fit current constants from the CON2020 model as a function of Juno orbit number. Solid red and blue lines show the best fit azimuthal ($\frac{\mu_0 I_0}{2}$) and radial ($\mu_0 I_{rad}/2\pi$) current constants, respectively, obtained via the method described in the text. The dashed lines show the best fit current constants derived by Connerney et al. (2020). (bottom) The RMS error in $|B|$ as a function of Juno orbit number.

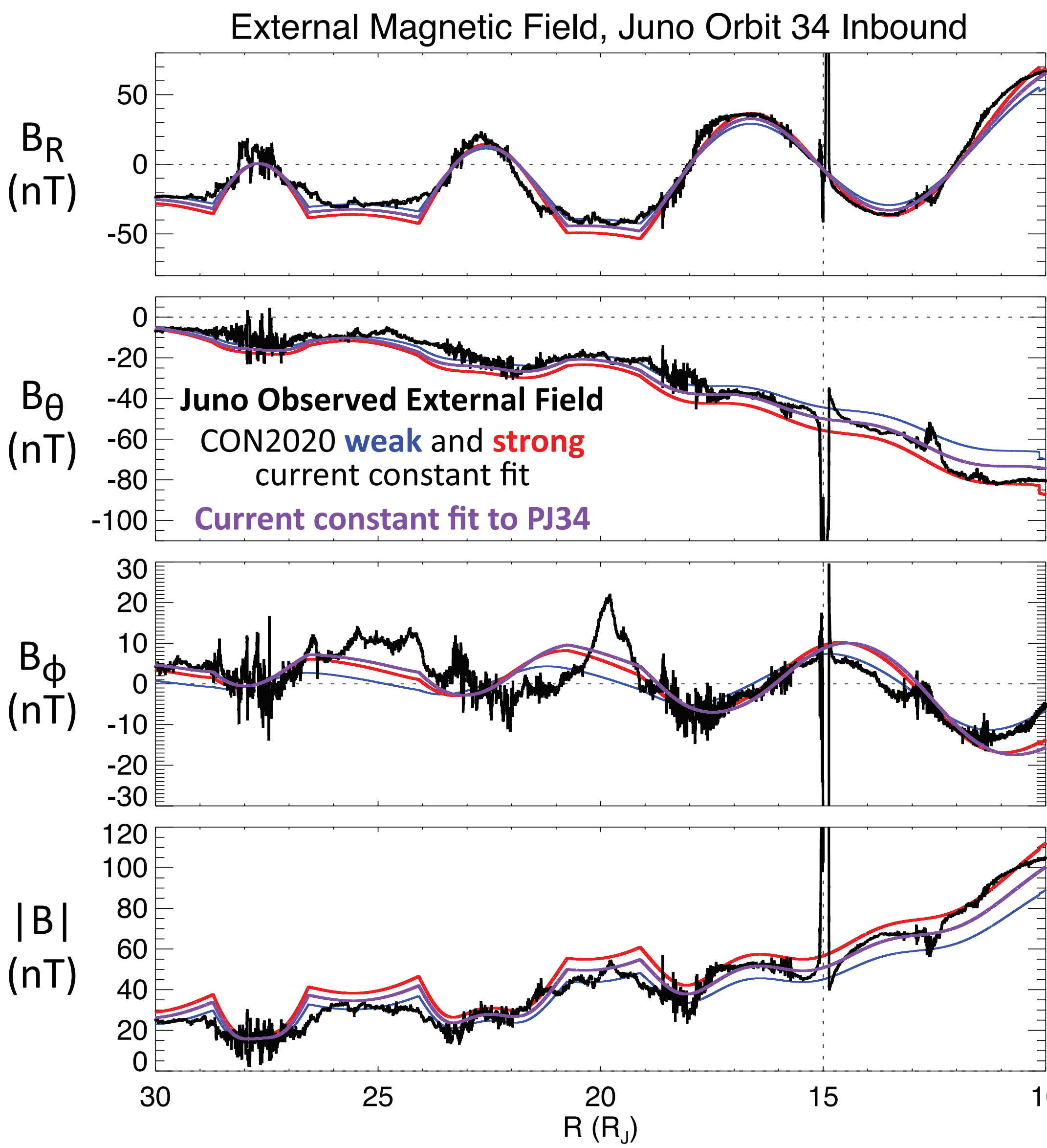


**Figure S6.** The external magnetic field (observed field – JRM09 internal field model) as a function of spherical radial distance during Juno's inbound orbit 34. Black lines show the measured magnetic field, red and blue lines show the CON2020 model fits assuming the strongest and weakest current constants fit by Connerney et al. (2020) to Juno's first 24 orbits. Purple lines show the CON2020 field calculated using the best fit current constants we calculated for Juno orbit 34 ($\frac{\mu_0 I_0}{2}$ = 138 nT, $\mu_0 I_{rad}/2\pi$ = 44 nT).

**Table 1.** Measured and modeled magnetic field values and field angles near Ganymede's orbit

| | Minimum (excepting orbit C9[a]) | Maximum (all orbits) | Minimum (Orbit C9 only[a]) | JRM09 + CON2020 model minimum[b] | JRM09 + CON2020 model maximum[b] | JRM09 + CON2020 model average[b,c] | Average variability due to change in CON2020 current constants[c] |
|---|---|---|---|---|---|---|---|
| $B_R$ (nT) | -92.78 | 95.15 | | -83.80 | 85.61 | 53.9 | ~6 nT |
| $B_\theta$ (nT) | 48.50 | 105.50 | 32.06 | 69.54 | 78.55 | 74.36 | ~11 nT |
| $B_\varphi$ (nT) | -21.91 | 25.12 | -27.10 | -14.28 | 15.83 | 9.47 | ~2 nT |
| $\|B\|$ (nT) | 63.76 | 126.59 | 37.24 | 70.76 | 116.2 | 94.95 | ~5 nT |
| Bendback angle[d] (degrees) | -82.43 | 82.06 | | -88.43 | 86.62 | 17.39 | ~4° |
| Elevation angle[d] (degrees) | 33.75 | 88.61 | | 42.15 | 89.72 | 56.30 | ~6° |

[a] The magnetic field measured during orbit C9, which occurred near 50° longitude, was anomalously small due to a likely current sheet crossing, which affects the minimum observed $B_\theta$, $B_\varphi$, and $|B|$.

[b] Model values were calculated at 15.0 $R_J$, 0° latitude, and from 0° to 360° longitude in 1° increments, using the average CON2020 current constant fit values.

[c] Averages and variability are calculated using $|B_R|$, $|B_\varphi|$, and the magnitude of the field bendback angle.

[d] Field angles are not calculated when $|B_R| < 3$ nT.

**Table 2.** JRM09 + CON2020 model prediction at Ganymede's orbit[a] during the Juno flyby

| | 50º longitude, average | 50º longitude, expected temporal variability | 70º longitude, average | 70º longitude, expected temporal variability |
|---|---|---|---|---|
| $B_R$ (nT) | -28.3 | -29.6 – -27.1 | -1.1 | -0.7 – -1.4 |
| $B_\theta$ (nT) | 69.9 | 64.1 – 75.3 | 69.6 | 63.7 – 75.2 |
| $B_\varphi$ (nT) | -10.2 | -8.7 – -11.4 | -11.5 | -11.7 – -13.4 |
| $\lvert B \rvert$ (nT) | 76.1 | 71.2 – 80.8 | 72.1 | 64.8 – 76.3 |
| Bendback angle | 19.9º | 16.3º – 22.8º | 37.5º | 86.6º – 84.1º |
| Elevation angle (degrees) | 67.9º | 65.2º – 70.2º | 77.9º | 89.4º – 88.9º |

[a]Model field computed at 15 $R_J$ radial distance and 0º jovigraphic latitude

**Figure 1.**

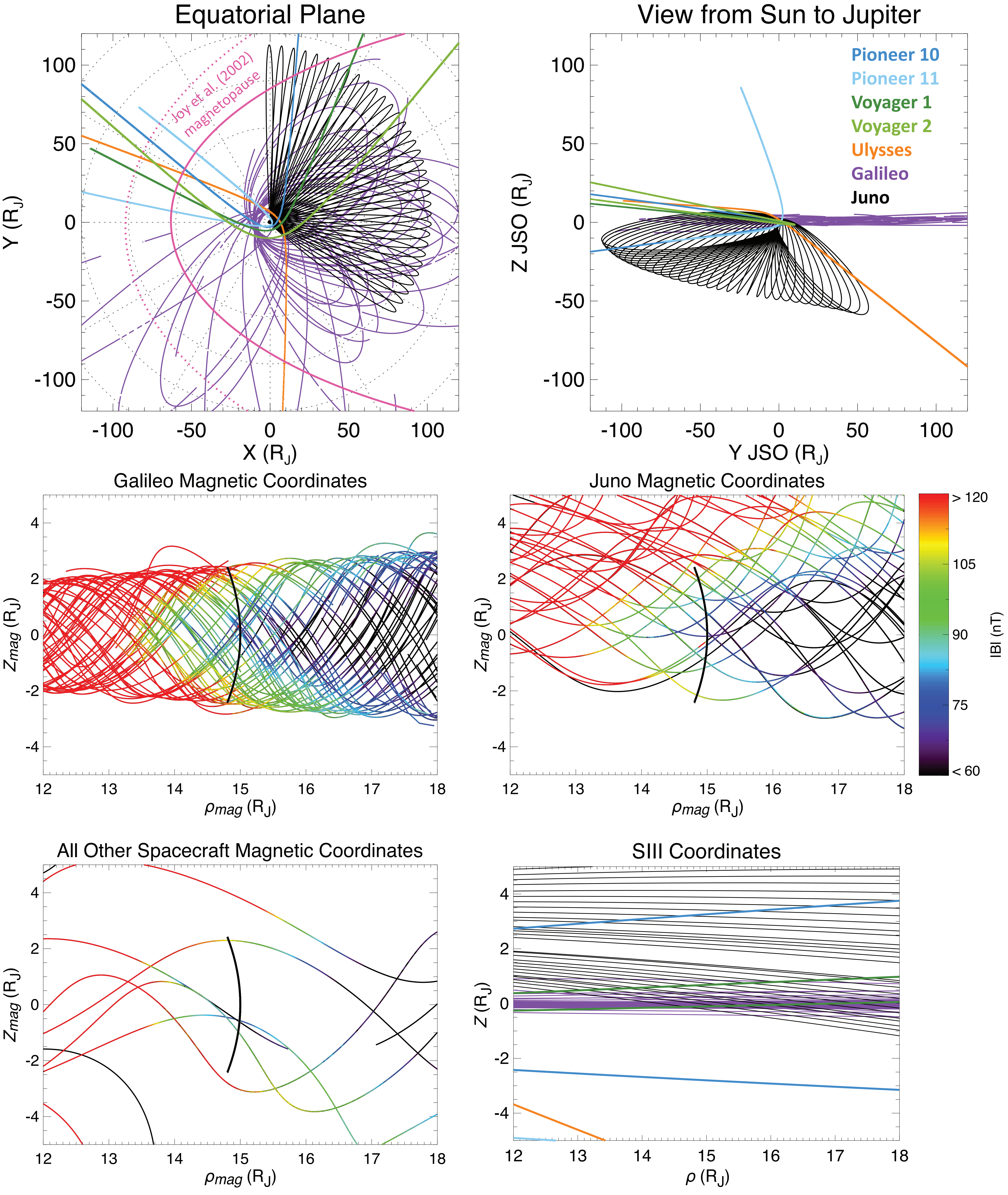

Equatorial Plane
Joy et al. (2002) magnetopause
Y (R_J)
X (R_J)
View from Sun to Jupiter
Pioneer 10
Pioneer 11
Voyager 1
Voyager 2
Ulysses
Galileo
Juno
Z JSO (R_J)
Y JSO (R_J)
Galileo Magnetic Coordinates
Juno Magnetic Coordinates
> 120
105
90
75
< 60
|B| (nT)
$Z_{mag}$ (R_J)
$\rho_{mag}$ (R_J)
All Other Spacecraft Magnetic Coordinates
SIII Coordinates
Z (R_J)
ρ (R_J)

**Figure 2.**

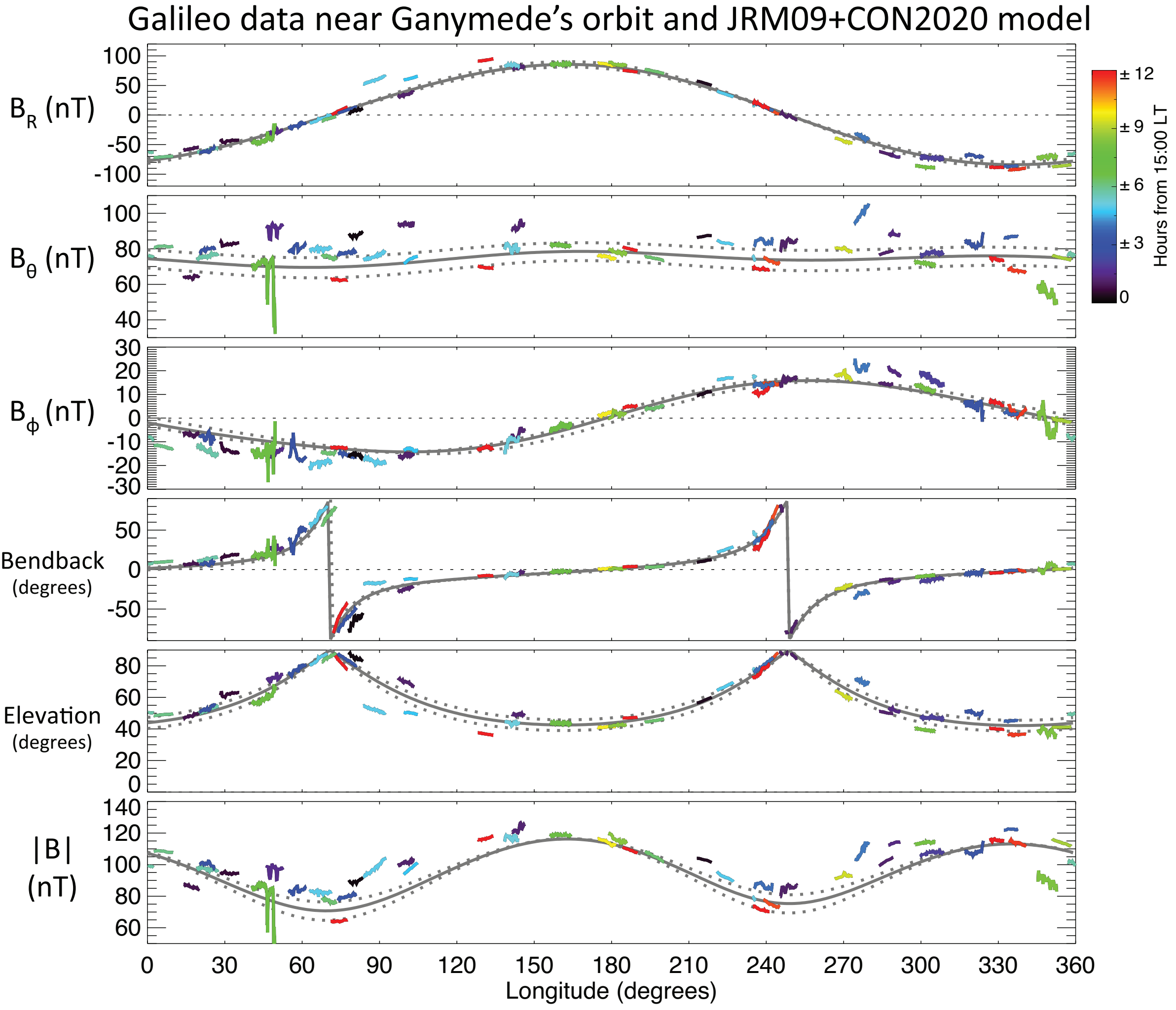
Galileo data near Ganymede's orbit and JRM09+CON2020 model
$B_R$ (nT)
$B_\theta$ (nT)
$B_\phi$ (nT)
Bendback (degrees)
Elevation (degrees)
|B| (nT)
Longitude (degrees)
Hours from 15:00 LT
± 12
± 9
± 6
± 3
0

**Figure 3.**

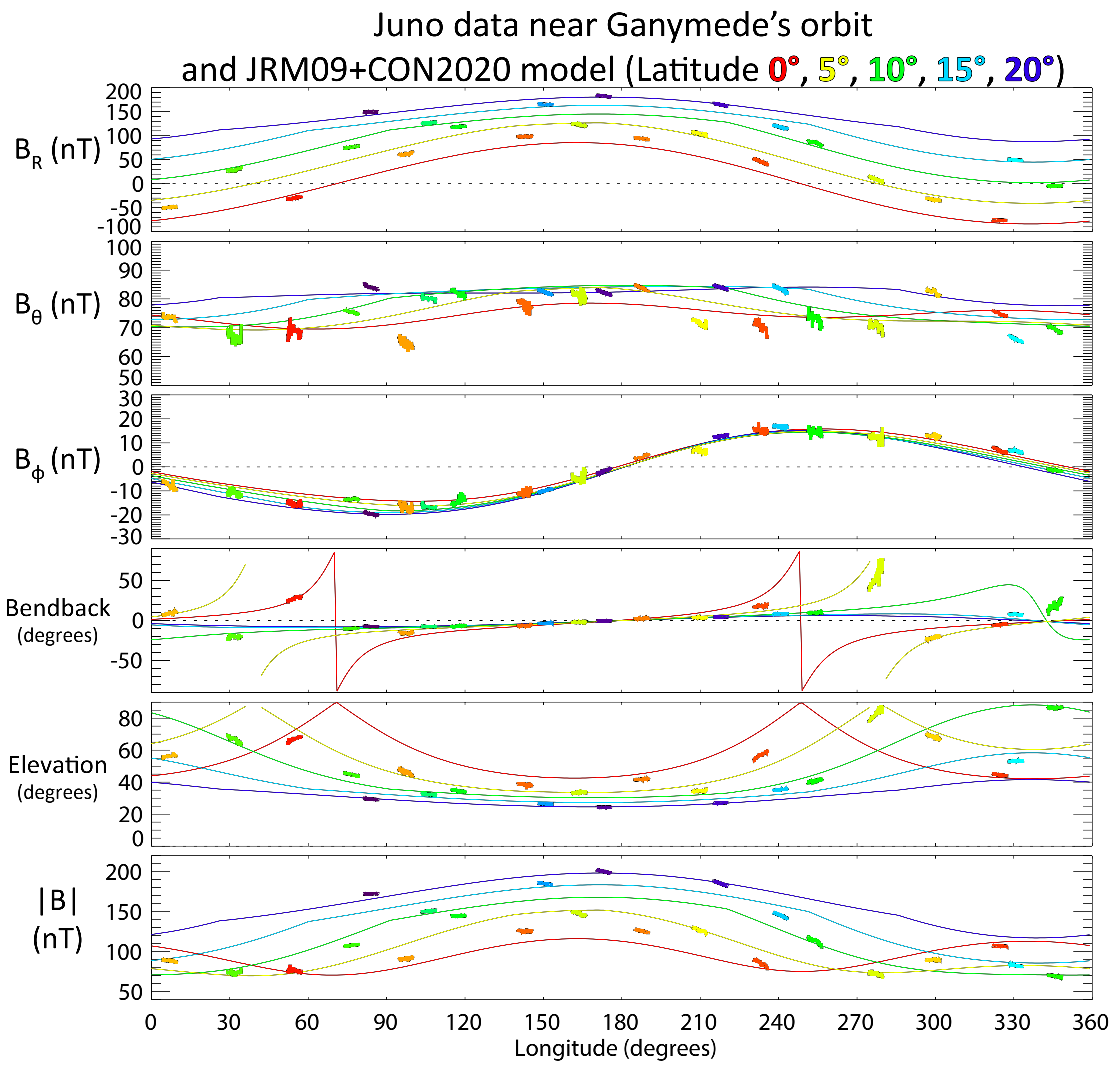
Juno data near Ganymede's orbit
and JRM09+CON2020 model (Latitude 0°, 5°, 10°, 15°, 20°)
B_R (nT)
B_θ (nT)
B_φ (nT)
Bendback
(degrees)
Elevation
(degrees)
|B|
(nT)
Longitude (degrees)

**Figure 4.**

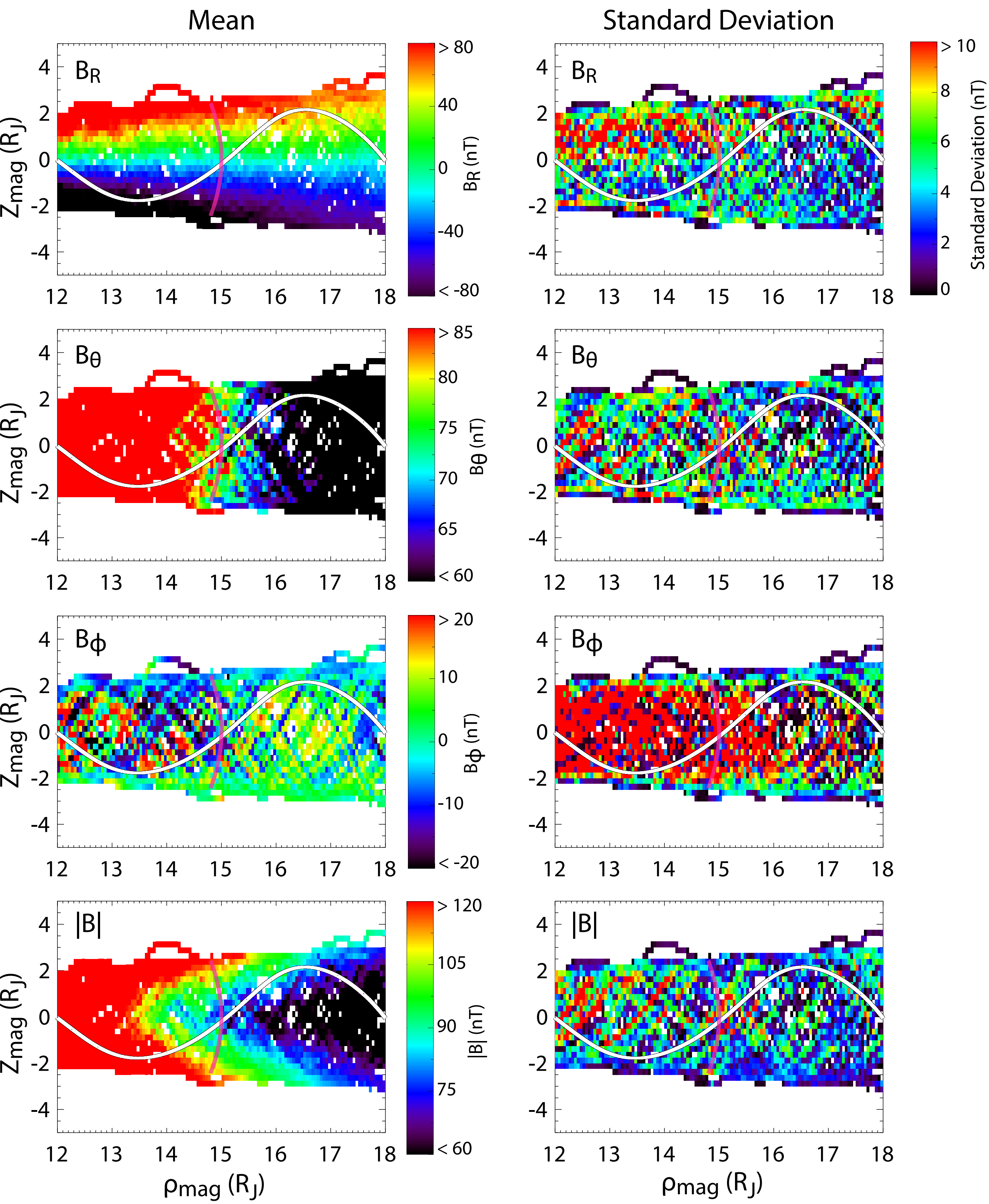

Mean
Standard Deviation
B_R
B_θ
B_φ
|B|
Z_mag (R_J)
ρ_mag (R_J)
B_R (nT)
Bθ (nT)
Bφ (nT)
|B| (nT)
Standard Deviation (nT)
> 80
40
0
-40
< -80
> 85
80
75
70
65
< 60
> 20
10
0
-10
< -20
> 120
105
90
75
< 60
> 10
8
6
4
2
0

**Figure 5.**

**Juno Measured Field**, **Galileo Average**, and **JRM09+CON2020 model** along Juno's orbit